



Research Article

<https://doi.org/10.1631/jzus.A2500344>

Hierarchical learning method for array flow field prediction integrated with deep neural network

Shanxun SUN¹, Zijiang XU¹, Zhuoheng WANG¹, Shuangshuang CUI², Ting HE¹✉, Yang CAI¹✉

¹Energy and Electricity Research Center, Jinan University, Zhuhai 519070, China

²Guangdong-Hong Kong-Macao Greater Bay Area Meteorological Intelligent Equipment Research Center, Guangzhou 511430, China

Abstract: Real-time and accurate dynamic wake information is essential for wind resource assessment and the optimization of wind farm operations. To further understand the wake characteristics of wind turbines, we propose a hierarchical learning approach integrated with a deep neural network-based prediction method. The integrated framework combines physical and mathematical models, enabling three-dimensional spatiotemporal wind field predictions with minimal measured data requirements. Evaluation and validation results demonstrate that the proposed method achieves accurate short-term wake predictions across the entire domain with minimal prediction errors. Compared with conventional methods, the proposed hierarchical learning framework markedly lowers the training-data requirements of physics-informed neural networks for large-scale flow-field prediction while maintaining high accuracy. In addition, it demonstrates superior performance in both local and global wake forecasts, offering practical insights for efficient turbine operation and wake analysis.

Key words: Hierarchical learning; Integrated neural network; Wind farms; Ultra-short-term wake prediction

1 Introduction

With the continuous global expansion of wind power capacity, the impact of wake effects on electricity production has become increasingly significant and must be addressed. Studies indicate that wake effects can result in a 10%-40% power loss in wind farms and significantly increase fatigue damage to downstream wind turbines (Wang et al., 2024b). Therefore, effectively harnessing wind resources and wake effects have emerged as critical research challenges in the field of wind energy. Approaches to address these issues include optimizing wind turbine layouts in large-scale wind farms and implementing active wake control strategies during operation. However, substantial difficulties exist in precisely assessing and modeling

wind farm wakes, stemming from temporal and spatial variations in wind velocity, nonlinear wake interactions between turbines, and turbulent atmospheric conditions.

In practical applications, significant research efforts have been devoted to developing methods for reconstructing and predicting wind turbine wake fields. The current methodologies for predicting wake fields can be systematically categorized into three distinct groups: analytical wake models, computational fluid dynamics-based simulations, and machine learning-enhanced approaches. Analytical models such as the Jensen model (Jensen, 1983), Frandsen model (Frandsen et al., 2006), Bastankhah model (Bastankhah et al., 2014), and 3D wake models (He et al., 2021) are widely used for rapid prediction, yet they have limited data accuracy. This phenomenon can be attributed to inflow conditions and local environmental factors that influence wake fields. These factors are often not accounted for in analytical models, which are typically limited to modeling the wakes of individual wind turbines. In contrast, CFD models provide higher prediction accuracy and can simulate wake fields of wind

✉ Ting HE, heting@jnu.edu.cn

Yang CAI, thomascai301@163.com

Shanxun SUN, <https://orcid.org/0000-0001-9297-685X>

Received July 24, 2025; Revision accepted Dec. 29, 2025;
Crosschecked

turbines in complex terrains. However, in large-scale wind farms with intricate and interconnected turbine layouts, substantial computational resources including CPU and memory are required.

In recent years, advancements in data science and artificial intelligence technologies have driven significant progress in the application of machine learning methods for predicting wind turbine wake fields. Some models have incorporated turbulence effects (Purohit et al., 2022), yawed wake effects power prediction (Sun et al., 2020), and even integrated high-fidelity data (Li et al., 2023). However, machine learning approaches are often data-driven, requiring large volumes of high-quality data for model training, and often suffer from limited interpretability. Hybrid methodologies integrate the complementary advantages of distinct approaches to enhance predictive accuracy while maintaining error tolerances consistent with their constituent methods. Techniques such as orthogonal decomposition reduce the dimensionality of high-dimensional flow field data, and long short-term memory (LSTM) networks predict dimensionality reduction coefficients, enabling rapid reconstruction of wake fields in large wind farms within seconds (Zhou et al., 2023).

Using numerical simulations of wind farms to drive deep neural networks (DNNs) for wake field prediction has emerged as a predominant research methodology. A wind-pumped storage-hydrogen energy combined operation system based on deep learning was proposed providing valuable insights into wake effect modeling and prediction for wind farms (Wang et al., 2023). Large Eddy Simulation (LES) has been used to generate high-precision wake and output power data. When combined with a multi-task CNN model to simultaneously predict wake velocity, wake turbulence intensity, and output power, this approach captured the potential dependencies between these variables and improved prediction accuracy (Songyue et al., 2025). A Dual-Adaptive Multi-Fidelity Neural Network framework was proposed to solve the negative migration phenomenon of Multi-Fidelity Neural Networks when combining CFD simulation data by introducing an Adaptive Multi-Fidelity module and an Adaptive Fast Weighting module. This significantly improves the accuracy of wake prediction and the efficiency of data utilization (Zhan

et al., 2024). Light detection and ranging (LiDAR) have been used to build a wake prediction framework together with a Physical Informed Neural Network (PINN) and has significantly improved prediction accuracy and training efficiency through spatial and temporal improvement strategies (Song et al., 2025). Similarly, by combining LiDAR and physical information neural networks, real-time dynamic wake field reconstruction has been achieved for yaw control in wind farms (Wang et al., 2024a). Additionally, a method of wind field reconstruction using CFD and Proper Orthogonal Decomposition (POD) with optimal sensor placement was proposed by Sun et al. (2019).

However, this research did not consider that the implementation of DNN for wake prediction requires numerical methods to provide a substantial volume of data, which inherently increases algorithmic complexity. Consequently, the feasibility of such approaches in real-world wind farm applications remains to be thoroughly evaluated.

Layered learning, widely applied in intelligent optimization and control, data mining, and deep learning, shows excellent performance in handling large-scale data and complex tasks (Sun et al., 2018). Real-time and precise wake prediction is crucial for the stable operation of wind farms. We propose a layered learning-based ensemble approach for predicting wakes of wind turbines in large-scale wind farms. By using a hierarchical learning approach to capture both global and local variations in wind farm wake fields, the proposed method effectively reduces the data requirements of a physics-informed neural network for large-scale flow field prediction while maintaining high predictive accuracy, thereby achieving precise prediction of the entire wind farm. This method can be applied to wake prediction studies in large-scale wind farms, providing high spatiotemporal resolution for both local and global wind farm conditions. It is suitable for challenging environments, such as large offshore wind farms and wind farms in complex terrains, and for applications including wind resource assessment and wake control.

2 Framework based on hierarchical learning

Conventional deep learning architectures

typically demand substantial training datasets, derived mainly from either computationally intensive high-fidelity simulations or comprehensive historical measurement campaigns to guarantee model accuracy and robustness. As the volume of data increases during actual training, the time and cost of training also rise, making model tuning more challenging. In this study, we propose a layered learning approach based on physics-informed neural networks, which reduces the volume of input training data while enhancing the accuracy and computational speed of prediction of wake fields in wind farms.

2.1 Integrated neural network framework

To balance prediction accuracy and model responsiveness, the proposed flow field reconstruction method is built on a DNN framework known as the Physics-Informed Neural Network (PINN). This framework consists of two feedforward neural networks: a Data Neural Network (Data-NN) for fitting the data, and a Partial Differential Equation Neural Network (PDE-NN) incorporating the Navier-Stokes (NS) equations (Fig. 1). Initially, a foundational DNN, Data-NN, is constructed using an offline database that includes historical measurement data and supplementary simulation data. Subsequently, the PDE-NN is derived from the Data-NN. The Data-NN is trained to fit sparse wake information inputs, while the PDE-NN is constructed by automatically differentiating the three-dimensional NS equations using the output of the Data-NN.

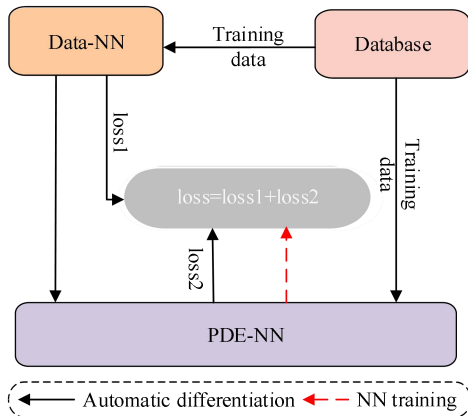


Fig. 1 A method for predicting the spatiotemporal wake flow using a combined model for wake prediction

A fully connected neural network architecture, designated as the Data Neural Network (Data-NN;

Fig. 2) and denoted as F , normalizes the data. Data-NN establishes a mapping between non-dimensionalized spatiotemporal coordinates $X = [t, x, y, z]$ (representing temporal and three-dimensional Cartesian spatial coordinates) and non-dimensional state variables $Y = [u, v, w, p]$ (where u, v , and w denote velocity components along x, y , and z axes respectively, and p represents pressure). The input to the network is the non-dimensional spatiotemporal coordinate set $X = [t, x, y, z]$. This set forms the minimal and fundamental input required by the PINN framework. The inclusion of time t allows the model to learn the transient dynamics of the flow, while the three-dimensional spatial coordinates $[x, y, z]$ enable the reconstruction of the complete volumetric flow field. The output $Y = [u, v, w, p]$ is thus a function of this continuous input space, $Y = F(X)$, allowing for prediction at any arbitrary location and time within the simulated domain. For ease of encoding partial differential equations (PDEs) in subsequent steps, the Data-NN outputs include pressure p ; however, training and fitting of pressure p are not conducted within the Data-NN. Given spatiotemporal coordinates $X = [t, x, y, z]$ at any time point, the trained Data-NN outputs state variables $Y = [u, v, w, p]$, which can be used to derive and encode subsequent calculations.

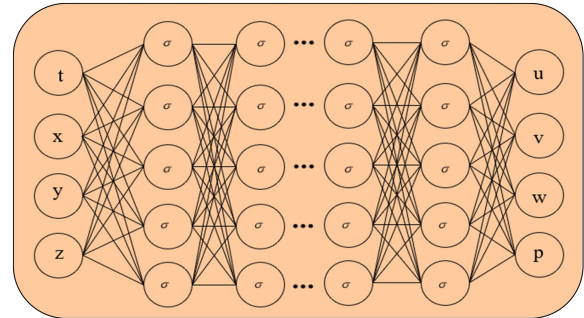


Fig. 2: Data-NN

Based on the description above, the fully connected Data-NN can be represented by (1):

$$\begin{aligned}
 H_0 &= [t, x, y, z], \\
 H_i &= \sigma(H_{i-1} \cdot W_i + B_i), \\
 H_L &= [u, v, w, p],
 \end{aligned}
 \tag{1}$$

where $L+1$ represents the total number of layers in the Data-NN, $1 \leq i \leq L$, and $\{W_i\}$ and $\{B_i\}$ denote all trainable variables in this neural network. W_i represents weight matrices, B_i represents bias terms, and σ denotes the activation function. If h denotes the

number of neurons in the hidden layer, then the shapes of the weight matrices W_1 , $\{W_i\}$, and W_L are $[4, h]$, $[h, h]$ and $[h, 4]$, respectively. The shapes of the bias terms $\{B_i\}$ and B_L are $[1, h]$ and $[h, 4]$, respectively.

For the activation functions, $\{\sigma_i, 1 \leq i \leq 3\}$, $\{\sigma_i, 4 \leq i \leq 5\}$, and $\{\sigma_i, 5 < i\}$, they are respectively hyperbolic tangent functions, Relu functions, and hyperbolic tangent functions. To effectively capture turbulent effects and variations in flow fields, models often require substantial input data during training, which significantly increases computational time. Therefore, using the Relu activation function in specific hidden layers can reduce the model's iteration time by about half. The total degrees of freedom of the Data-NN, i.e., the total number of trainable variables, can be calculated using (2):

$$N_{dof} = 4h + (L - 2)hh + 4h + (L - 1)h + 4 \quad (2)$$

In the Data-NN, N_{dof} represents all trainable variables. Therefore, $Y = F(X; N_{dof})$, and the Data-NN is trained by minimizing the squared difference between the predicted output Y and the target training data.

Here, the PDE-NN encompasses the 3-dimensional Navier-Stokes equations describing fluid motion, derived through a combination of Data-NN and partial differential equations (Fig. 3), denoted as F_{ns} . It shares the same trainable variables as the Data-NN. The NS equations are effective in describing aerodynamics. The physics-informed deep learning framework is used to solve forward and inverse problems involving nonlinear PDEs, leveraging the synergy between physics and data. This approach has achieved significant success across various domains (Zhang and Zhao, 2021; Sun et al., 2024). For wind field reconstruction, the 3-D NS equations can be rewritten as shown in Section S1 of the electronic supplementary materials (ESM).

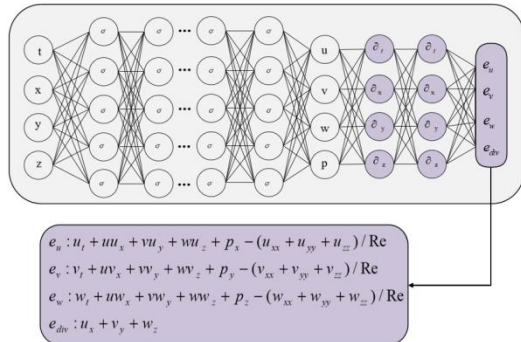


Fig. 3 The framework of PDE-NN

The residual term in the PDE-NN consists of the 3D NS equations. The differential terms are obtained through automatic differentiation of the output from the Data-NN, with higher-order terms derived from lower-order terms through automatic differentiation. The PDE-NN is represented as F_{ns} , thus its output is $Y_{ns} = F_{ns}(X_{ns}; [W, 1/Re])$, where the input $X_{ns} = [t, x, y, z]$. Therefore, the PDE-NN can be re-expressed as (3):

$$Y_{ns} = F_{ns}(X_{ns}; [N_{dof}, 1/Re]) \quad (3)$$

During the reconstruction process, the two sub-frameworks share the same training variables N_{dof} . The training procedure for the PINN involves two steps:

- 1) Updating N_{dof} and $1/Re$;
- 2) Minimizing the loss function of the PINN.

During training, the PDE-NN and Data-NN share the same database. The loss function of the composite model must incorporate the residual constraints of the 3D NS equations to ensure physical consistency and accurately capture fluid dynamics phenomena. Simultaneously, the loss function must account for fitting losses imposed by the training database to ensure effective fitting and generalization on the given datasets.

To meet the residual constraints of the 3D NS equations and simultaneously fit the training data, the loss function is decomposed into $L_1(N_{dof})$ and $L_2(N_{dof}, 1/Re)$ terms, as shown in (4) and (5):

$$L_1 = \frac{1}{N^d} \sum_{i=1}^{N^d} |F_d(t_i^d, x_i^d, y_i^d, z_i^d, N_{dof}) - u_i^d|^2 \quad (4)$$

$$L_2 = \frac{1}{N_{ns}} \sum_{i=1}^{N_{ns}} |F_{ns}(t_i^{ns}, x_i^{ns}, y_i^{ns}, z_i^{ns}; [N_{dof}, 1/Re])| \quad (5)$$

In (4), $\{[t_i^d, x_i^d, y_i^d, z_i^d, u_i^d], 1 \leq i \leq N_d\}$ represents the training database consisting of spatiotemporal coordinates and corresponding wind velocities. In (5), $\{[t_i^{ns}, x_i^{ns}, y_i^{ns}, z_i^{ns}], 1 \leq i \leq N_{ns}\}$ represents a small amount of discrete real-time measurement data and corresponding spatiotemporal coordinates.

Subsequent computations require non-dimensionalization of the obtained data based on characteristic units. The loss function is defined in (6) with the corresponding spatiotemporal coordinates.

$$L(N_{dof}, 1/Re) = L_1(N_{dof}) + L_2(N_{dof}, 1/Re) \quad (6)$$

2.2 Model framework based on hierarchical learning

In large-scale wind farms, variations in wind speed and wake effects significantly affect wind turbine operation. Downstream turbines located within the zone of influence of upstream turbines experience wake effects, resulting in increased fatigue damage and a reduced operational lifespan.

For wake prediction, to reduce the amount of training data and improve prediction accuracy, we constructed a hierarchical learning model (Fig. 4). The model comprises two components: a small-scale PINN designed to capture wind speed patterns in densely populated regions, and a large-scale PINN tailored to fit sparse data points across the entire wind farm. Unlike generic hierarchical models, the proposed framework is specifically engineered for the wind farm wake prediction problem. The hierarchical sampling is driven by the flow acceleration, a direct proxy for the complex wake dynamics we aim to capture. The integration of the NS equations ensures that the model adheres to the underlying physics, making it well suited for predictions with sparse measurement data. The small-scale PINN learns the localized variations in the wind farm, while the large-scale PINN considers the turbulent trends of the entire wind farm. These PINNs are the combined prediction models developed in Section 2.1, enabling precise forecasting of the entire wind farm.

The hierarchical learning model (Fig. 4) consists of two parts: a small-scale PINN and a large-scale PINN. Data from the wind farm database are filtered based on wake-induced wind speed variations, with the blue regions containing more pronounced variations used as training data to minimize $Loss_{data1}$. This yields a localized wake prediction model tailored to the wind speed variations in those areas. For regions with fewer wind speed variations, represented in gray, a random selection of one-tenth of the data is used as training data to minimize $Loss_{data2}$. This results in a wake prediction model that fits the overall wind speed patterns across the wind farm. The combination of these two wake prediction models yields a final model specific to the wind turbine array.

The hierarchical learning model uses acceleration to filter relevant feature data during data processing. This approach has similarities to the Adaptive Mesh Refinement (AMR) technique

commonly used in CFD, especially in refining the resolution of regions with steep gradients or fast changes. AMR typically involves adaptive grid refinement based on predefined criteria across the entire domain, whereas our approach dynamically adjusts the resolution only at localized points where there are significant changes in gradients or accelerations. In other words, our hierarchical approach is more like the Gradient-based One-Side Sampling in the lightGBM method in terms of understanding. By not changing the distribution of samples, hierarchical sampling of training data not only does not reduce model performance, but also increases the diversity of weak learners, potentially improving the model's generalization ability.

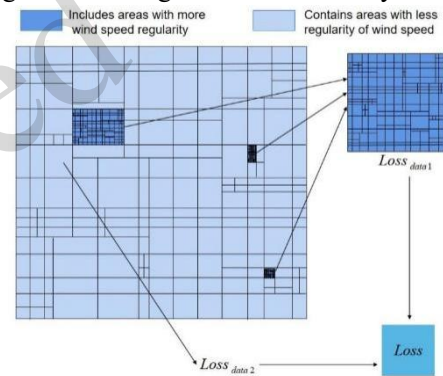


Fig. 4 Hierarchical learning model based on the PINN

Data points with acceleration above a certain fixed threshold are retained entirely, while those below the threshold have one-tenth of their data selected. The processed data are then separately input into small-scale and large-scale PINNs, which share a similar structure to the PINN architecture developed in Section 2.1. To simplify the model structure and reduce computational costs, these two models are merged into a single neural network and trained to minimize the neural network loss function, 'Loss'. During training, the hierarchical learning model uses processed wind farm coordinates as input and minimizes the 'Loss' function. Throughout the training process, the 'Loss' function decreases and eventually stabilizes, fluctuating slightly around a fixed value. Training times initially exhibit variability but eventually stabilize, thereby reducing computational requirements.

Upon completion of training, the proposed prediction method not only optimizes data resource utilization but also reduces computational costs,

thereby providing a reliable approach for flow field reconstruction and forecasting in large-scale, complex wind farm environments.

To effectively reduce the amount of training data required and improve wake prediction accuracy, we constructed a hierarchical learning-based wake prediction model, whose overall framework is shown in Fig. 5. Through a hierarchical sampling strategy based on an acceleration threshold, the model retains all data in high-dynamic regions while randomly selecting only one-tenth of the data from regions with mild variations for training. Finally, the two-scale PINNs are integrated into a single network for joint training to minimize the overall loss function, thereby achieving efficient and accurate prediction of wind farm wakes.

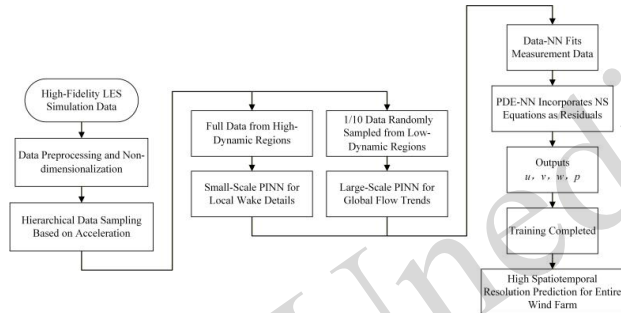


Fig. 5 Framework of the hierarchical learning model for wake prediction

3 Simulation and validation

To rigorously validate the model's predictive accuracy, it is imperative to construct a comprehensive training database encompassing multi-condition wind speed distributions. This dataset functions as the foundational input for both model training and subsequent wake condition predictions across the wind farm. First, comprehensive geospatial data of the wind farm must be archived, including high-resolution terrain elevation, surface roughness characteristics, and surrounding obstacle distribution. These geographical parameters are fundamental for accurate wind field simulation. Based on the actual wind farm scenario, software settings must be adjusted to ensure consistency between the simulation setup and the real-world measurements, thereby improving the reliability and accuracy of the model. However, the acquisition of accurate historical data remains technically challenging, due mainly to terrain complexity and inherent limitations in measurement

instrumentation precision. Therefore, during the actual model training process, high-fidelity simulation data are used as a substitute for historical data to approximate real wind field conditions as closely as possible. This approach enhances model training and improves its performance and accuracy in practical applications.

The high-fidelity Large Eddy Simulation (LES) solver in OpenFOAM has been extensively used for numerical simulation and validation in studies of atmospheric boundary layer inflow and wake effects in wind farms. During the simulation, atmospheric boundary layer conditions with unstable convection are configured, using an actuator line model combined with LES method to investigate wake effects in wind farms. To more accurately simulate real wind farms and align with measured data, inputs such as inflow wind speed and direction are adjusted based on partial data from 3D radar and mast measurements. During the configuration phase, iterative calibration procedures are implemented to optimize both the wind farm simulation parameters and radar measurement data to ensure alignment between simulated data and real measurements, thereby improving the reliability and accuracy of the simulation results.

The NREL 5 MW wind turbine is a widely used publicly available wind turbine design for numerical simulation studies, developed by the National Renewable Energy Laboratory for performance evaluation and research in wind farms (Xu et al., 2024). Section S2 of the ESM lists the basic parameters of this wind turbine.

The numerical simulation is conducted in two steps (Fig. 6). The precursor atmospheric boundary layer simulation establishes physically consistent inflow conditions, with the output database serving as prescribed inlet boundary conditions for the main simulation. Subsequently, the wind turbine wake model is integrated into the main simulation using an actuator line model to simulate and compute the wake effects of wind turbines under the corresponding atmospheric boundary layer inflow conditions (Amiri et al., 2024).

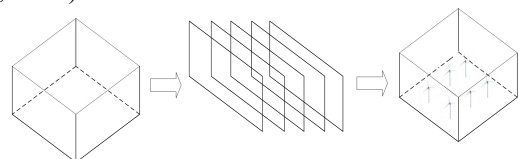


Fig. 6 Diagram of the Numerical Simulation Process

3.1 Precursor simulation

First, the precursor atmospheric boundary layer simulation is configured to simulate airflow dynamics, turbulent coherent structures within the atmospheric boundary layer, and their interactions with the Earth's surface. To match actual wind farm conditions, parameters in the simulation need adjustment. This includes wind speed, temperature, and turbulence parameters within the atmospheric motion equations, and the specification of boundary conditions such as terrain features and surface friction coefficients. Rational adjustment of these parameters improves the simulation's fidelity to observed data, enhancing accuracy and reliability.

In the precursor atmospheric boundary layer simulation, the wind farm was set to dimensions of 5.2 km in length, 2.6 km in width, and 1.01 km in height, with a grid resolution of 20 m. This resulted in 20 grids in each direction (x, y, z), totaling 1.706 million grids. The inflow wind direction was oriented at 254.48° to represent the predominant wind regime. The surface temperature flux (q_s) was set to $-0.04 \text{ K}\cdot\text{m/s}$ to simulate unstable convective atmospheric boundary layer flow. The initial potential temperature from the surface to a height of 0.9 km was set at 300 K, with a capping inversion layer from 0.8 to 1 km. The potential temperature increased linearly to 308 K above this layer, forming a cap over the computational domain to limit boundary layer expansion (Bai et al., 2023).

The precursor simulation prescribes an inflow wind speed of 11.4 m/s at the 90 m hub height, corresponding to typical rated turbine operation. Periodic boundary conditions were implemented laterally to maintain turbulence continuity throughout the computational domain, while a rigid no-slip condition with zero vertical velocity was enforced at the upper boundary. Surface friction effects were modeled using the Moeng wall formulation with a roughness length of z_0 set to 0.001 m, representing conditions typical of offshore wind farms. This setup emphasizes the impact of vertical convection on atmospheric structures under convective atmospheric conditions (Xu et al., 2023).

3.2 Main simulation

During the main simulation, it is crucial to consider the effect of complex terrain and turbine layout within the wind farm on airflow dynamics. Adjusting parameters such as grid resolution, turbine characteristics, and airflow boundary conditions enables a more accurate simulation of airflow distribution and turbulence structures within the wind farm. Additionally, factors such as the impact of turbine blades, tower structures on airflow, and interactions between turbines need careful consideration. Optimizing and adjusting these parameters enables more accurate and reliable simulation results of the internal flow fields within the wind farm, providing robust data support for subsequent hierarchical learning models.

The wind farm simulation models twelve sequentially arranged wind turbines using an actuator line approach to compute wake effects. The specific wind turbine layout for the wind farm is provided in Section S3 of the ESM. The main simulation uses the same computational domain size as the precursor atmospheric boundary layer simulation. Details are given in Section S4 of the ESM.

3.3 Verification of the proposed method

To validate the developed wake prediction model for large-scale wind turbine arrays, namely the hierarchical learning model based on the PINNs, a combination of Adam and Adadelta optimization algorithms was used for optimizing the hierarchical learning model. The training of the PINN within the hierarchical learning model was conducted using a GTX3050 GPU. The structure, along with the trained parameters of the PINN in the model, are presented in Section S5 of the ESM.

The trained hierarchical learning model captures rapid evolution details and turbulence characteristics from localized regions while learning the spatiotemporal correlations of wind farms based on the 3D-NS equations. Consequently, it enables precise reconstruction of the entire wind farm, or specific localized regions, for any given location, time and ultra-short-term wake predictions. This approach, which integrates local observations with global predictions, enhances both the scientific validity and predictive accuracy of the model.

For validation of the hierarchical learning model, the one-tenth of data was randomly selected to

reduce the training data volume. To capture temporal sequence information, wind farm data for a continuous 10s period were input into the hierarchical learning model to predict the wake field at the 11th second. The training dataset was derived from simulated wind farm data over the first 10s with a time interval of 1s, whereas the validation dataset comprised 3D radar and mast measurements from a real wind farm. Gaussian noise was added to the wind farm simulation data to replicate the measurement data to establishing the test database.

Upon completion of training the hierarchical learning model, given spatiotemporal coordinates $[t_i, x_i, y_i, z_i]$ where $i \in [1, 10]$, it becomes possible to reconstruct the wake field behind wind turbines. This enables the reconstruction of the wind farm by considering both localized fine wake and the overall flow field within the wind farm, combined with three-dimensional grid propagation, to effectively predict the wake field of the entire wind farm. This indicates that the model not only predicts the wake field of the entire wind farm but also achieves more accurate prediction of fine wakes in localized regions, thereby providing more reliable data support for wind farm operation and wind resource assessment.

To validate the proposed hierarchical learning model, the overall wake field of the wind farm was predicted, with detailed information provided in Section S6 of the ESM.

4 Results and discussion

4.1 Evaluation metrics

When assessing the predictive performance of a model, it is essential to use multiple evaluation metrics, as it can be challenging to comprehensively evaluate a model's performance based on a single error metric (Liu et al., 2023). Therefore, five metrics were used to assess the model's effectiveness: Maximum Error (ME), Minimum Error (me), Mean Absolute Error (MAE), Mean Relative Error (MRE), and Root Mean Square Error (RMSE).

4.2 Evaluation metrics

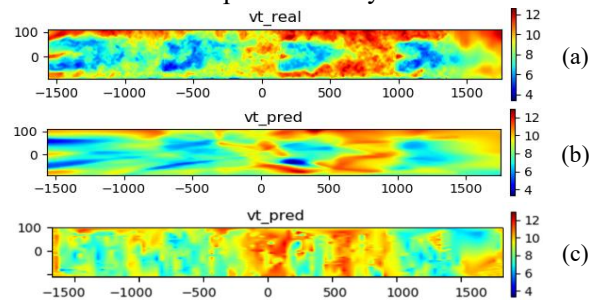
A comprehensive evaluation of the proposed model's predictive performance showed that the trained model can reconstruct large-scale wind farms in real time and predict the 3D spatiotemporal flow

field around wind turbines. The hierarchical learning model is trained using flow field information from any continuous time period within the training dataset. To compare and analyze prediction accuracy, flow field information from the first 10s, with a 1s interval, was selected to predict the wake field of an array of twelve wind turbines.

To further analyze the accuracy of the predicted flow field around the wind turbines, parallel cross-sections at the locations of the first, second and third rows of turbines were visualized. The numerical simulation results and wind farm predictions at the 11th second were calculated with MAEs of 0.214, 0.251 and 0.212, respectively.

In the overall prediction of the wind farm, areas with significant turbulence variations exhibited larger prediction errors. It suggested that focusing on learning the wind farm's dynamic patterns in regions with higher prediction errors will effectively reduce flow field prediction errors and enhance the accuracy of wind farm wake predictions.

To illustrate the improved wake prediction performance of the proposed method, we plotted the vertical resultant velocity contour maps at the coordinates of the wind turbines, covering three rows with four turbines per row, and compared them with the results from a Multilayer Perceptron (MLP) and a CNN. In Fig. 7, (a) shows the resultant velocity contour map of the first row of wind turbines (1, 4, 7, 10) from the numerical simulation, (b) shows the resultant velocity contour map predicted by the MLP for the first row, (c) shows the resultant velocity contour map predicted by the CNN, and (d) shows the resultant velocity contour map predicted by the hierarchical learning method. We used about one-third of the processed data to construct the database for overall wind farm prediction. Clearly, LSTM cannot achieve this functionality, so it was not included in the comparative analysis.



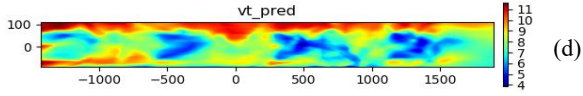


Fig. 7 Velocity contour maps of the first row of wind turbines (1, 4, 7 and 10)
(a) numerically simulated result; (b) predicted by MLP; (c) predicted by CNN; (d) predicted by the proposed method

As observed in Fig. 7, the proposed hierarchical learning method accurately predicted the wake behind the first row of wind turbines (1, 4, 7, and 10). The high-speed and low-speed flow structures surrounding each turbine were well-predicted, and the wind speed range was also predicted with reasonable accuracy. In contrast, the MLP and CNN failed to capture the local variation details in the wake, resulting in lower prediction accuracy and a larger overall prediction error. A careful observation of the high-velocity regions in Fig. 7(d), compared to the ground truth in Fig. 7(a), reveals a slight underestimation of the maximum velocity. This phenomenon can be attributed to the intrinsic physical constraints of the PINN framework. The residual terms of the NS equations enforce a solution that is globally smooth and physically consistent. While this ensures the overall stability and physical plausibility of the prediction, it may lead to a smoothing effect that dampens local extremes, particularly in regions with the sharpest velocity gradients. It is important to emphasize that this minor local discrepancy does not detract from the model's superior overall performance, as it still achieved the most accurate prediction of the wake structure and the lowest error metrics across all evaluated methods, as unequivocally shown in Table 1.

To further analyze the improvement in wake prediction performance by the hierarchical learning model, a mathematical analysis of the prediction results was conducted. Five error metrics for the cross-section predictions were used. Here, v_{t1} represents the resultant velocity predicted by the proposed method, while v_{t2} and v_{t3} represent the resultant velocity predicted by the MLP and CNN, respectively.

Table 1. Velocity Prediction Errors for the First Row

	<i>ME</i>	<i>me</i>	<i>MAE</i>	<i>MRE</i>	<i>RMSE</i>
v_{t1}	-0.301	0.410	0.311	0.0345	0.396
v_{t2}	0.346	-0.820	0.663	0.0771	0.887

$$v_{t3} \quad 1.420 \quad -1.584 \quad 0.637 \quad 0.0786 \quad 0.702$$

Table 1 shows the various error metrics for the resultant velocity predictions at the cross-sections of the first row of wind turbines (1, 4, 7 and 10) using the three methods. The proposed method shows superior predictive accuracy, exhibiting significantly reduced error metrics across all evaluation indicators compared to both MLP and CNN benchmarks. These results indicate enhanced prediction precision and overall performance improvement over conventional deep learning approaches. The larger predicted velocity errors of the MLP in Table 1 indicate its inability to capture the local and global wake dynamics within the wind farm, resulting in significant inaccuracies in wind speed predictions. The CNN, on the other hand, resulted in significantly higher maximum and minimum prediction errors for the closing speed than the other two methods due to its high sensitivity to the loss function.

Fig. 8 shows the velocity contour maps for the second row of wind turbines (turbines 2, 5, 8 and 11). The second row was significantly affected by the wake effects from the first and third rows. The proposed hierarchical learning model was capable of capturing the complex turbulence patterns and the dramatic wake variations around the turbines, accurately predicting wind speed even in regions with significant wake effects. In contrast, the MLP failed to capture the flow field variation patterns, resulting in a smaller predicted wind speed range and lower overall prediction accuracy. While the CNN captured the overall spatial distribution pattern of the wake region with reasonable accuracy, it exhibited significant limitations in quantitatively reproducing the wake's velocity deficit relative to the ambient flow conditions surrounding the turbine.

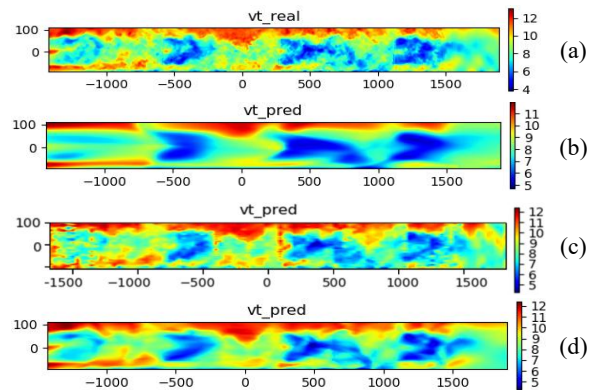


Fig. 8 Velocity contour maps of the second row of wind turbines (2, 5, 8 and 11)

turbines (2,5,8 and 11)

(a) numerically simulated result; (b) predicted by MLP; (c) predicted by CNN; (d) predicted by the proposed method

Table 2 shows that the proposed method yielded smaller error metrics across all indicators, and these errors were significantly lower than those produced by the MLP and CNN. The MLP and CNN exhibited larger maximum and minimum velocity errors, as they indiscriminately train on the input wind farm data. This broad training approach implies that while both methods attempt to capture the overall dynamics of the wind farm, they fail to accurately represent the localized turbulence structure changes, resulting in significant prediction errors in the details of local flow propagation.

Table 2. Velocity Prediction Errors for the Second Row

	<i>ME</i>	<i>me</i>	<i>MAE</i>	<i>MRE</i>	<i>RMSE</i>
v_{t1}	-0.433	0.390	0.297	0.0401	0.397
v_{t2}	-1.110	0.843	0.689	0.0821	0.855
v_{t3}	1.707	-1.579	0.447	0.0534	0.535

Fig. 9 presents velocity contour maps for the third row of wind turbines (3, 6, 9 and 12). The middle two turbines in this row experience a noticeable blockage effect, leading to lower wind speeds. The proposed hierarchical learning method also accurately predicted the wake in this region, with the wind speed range and values closely matching the true conditions. While the MLP correctly predicted the wind speed range, it exhibited a larger overall prediction error and lower prediction accuracy. While the CNN showed superior performance over the MLP, it exhibited systematic bias in predicting the wake's low-velocity regime and had inadequate sensitivity to wind speed variations in this region.

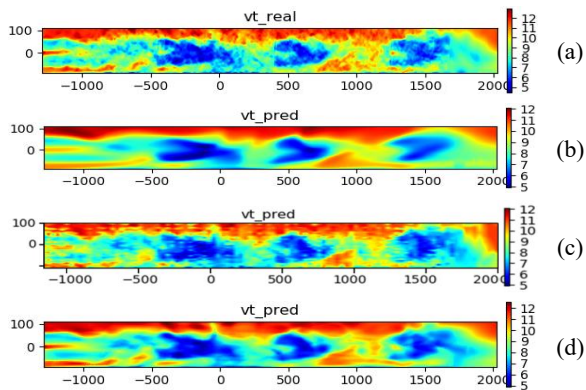


Fig. 9 Velocity contour maps of the third row of wind turbines (3, 6, 9 and 12)

(a) numerically simulated result; (b) predicted by MLP; (c) predicted by CNN; (d) predicted by the proposed method

Table 3 shows that the proposed method once again resulted in smaller error metrics across all indicators. The MLP showed a large absolute maximum velocity error and a small absolute minimum velocity error, indicating that its overall predicted range was excessively broad. The MLP does not specifically target the detailed wake regions where wind speed dynamics are complex, thereby failing to capture the intricate wake structure changes and resulting in larger prediction errors for the wake. The latter three metrics calculated for the CNN were superior to those of the MLP, but the overall error remained higher than that of our proposed method.

Table 3. Velocity Prediction Errors for the Third Row

	<i>ME</i>	<i>me</i>	<i>MAE</i>	<i>MRE</i>	<i>RMSE</i>
v_{t1}	-0.252	0.360	0.207	0.0251	0.452
v_{t2}	-0.861	0.478	0.263	0.0538	0.616
v_{t3}	1.506	-1.848	0.337	0.0404	0.439

Comparing the above results in Figs 7, 8 and 9, it is evident that regardless of the region, whether it is characterized by significant wake effects, pronounced blockage effects, or complex turbulence patterns, the proposed hierarchical learning method based on PINNs accurately predicts wind speed. The proposed method shows high-fidelity prediction of both high and low velocity flow structures around individual turbines, achieving superior accuracy in both wind speed magnitude and directional components. In comparison, the MLP shows significantly larger prediction errors, particularly in wake-affected regions with strong velocity deficits. In these areas, it predicts a narrower wind speed range with lower accuracy, despite requiring substantially more training data than the hierarchical learning model. From the prediction results in Fig. 7, it is evident that the CNN, as a purely data-driven model, produces predictions that do not conform to the physical laws of wake flow distribution when the data distribution is sparse.

The numerical analysis results indicate that for the second row of wind turbines, where wake effects are significant, and the third row, where blockage effects are pronounced, the proposed hierarchical learning model accurately predicted the wake with smaller overall prediction errors. In contrast, the

MLP’s prediction errors across the three tables did not show a clear numerical pattern, making it difficult to interpret the magnitude of the errors reasonably or to optimize the model parameters based on these errors to improve prediction accuracy. The predictive accuracy of the CNN showed strong dependence on input data distribution, limiting its capability to resolve the physical wake flow patterns with high fidelity. Comparative analysis confirmed the proposed model’s superior performance over both MLP and CNN approaches in terms of wake prediction accuracy and physical consistency.

This performance difference arises because the PINN framework in the hierarchical learning model implicitly considers the correlations between wind speeds at different locations through the residual terms of NS equations, thereby capturing the overall dynamics of the wind farm. Meanwhile, the Data-NN component specifically learns the fast-changing flow structures in regions with more turbulence. As a result, the model can accurately predict the local flow structures within the flow field.

The prediction results show that the hierarchical learning model, which selectively learns the overall wind farm dynamics and local flow details, not only significantly reduces the data required for model training but also enables accurate predictions of both global and local wake fields. Therefore, the proposed hierarchical learning model is capable of capturing wind farm dynamics, exhibiting excellent spatiotemporal prediction performance, and can be applied to ultra-short-term spatiotemporal wake prediction in wind farms. Note that although the proposed hierarchical PINN framework requires relatively high computational cost during offline training, the inference process is extremely fast once the model is trained. Therefore, the proposed method is applicable for short-term wake forecasting in practical wind farm operations.

In summary, the hierarchical learning model developed in this study outperforms the MLP and CNN in capturing the variations and details of the flow field, significantly enhancing the accuracy of wake prediction for wind turbine arrays.

To further assess the performance of the hierarchical learning model and illustrate its superiority in wind farm prediction, the third column of wind turbines was selected. A cross-section 441 m

downstream of this column, where the flow field exhibits more complex wind speed dynamics and larger data volume, was chosen for comparison. Additionally, the cross-section 441 m downstream of the fourth column, which also contains rich wind speed dynamics but with less data, was selected for further analysis. In Figs 10 and 11, (a) represents the velocity contour plot of the actual flow field obtained from numerical simulations, (b) shows the velocity contour plot predicted by MLP, and (c) shows the velocity contour plot predicted by CNN, (d) shows the velocity contour plot predicted by the hierarchical learning method. The visualization effects in the figures show that the overall flow structure and wind shear of the wind farm were well predicted. The predicted results also align more closely with the actual wind farm. This indicates that the proposed method successfully captures the three-dimensional spatial variations and temporal evolution of the incoming turbulent wind, demonstrating excellent spatiotemporal prediction performance.

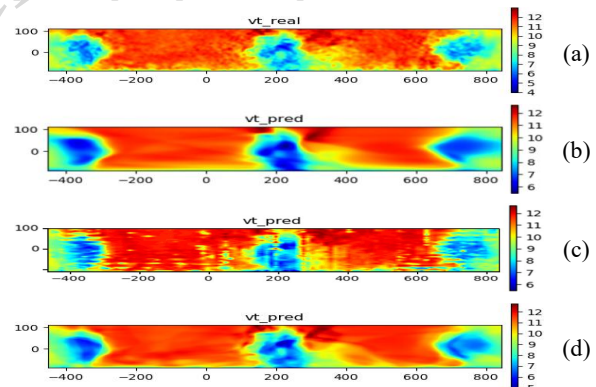


Fig. 10 Cross-section of the Flow Field 441 m downstream of the third column (turbines 7, 8, 9) of wind turbines (a) the actual flow field obtained from simulations; (b) predicted by MLP; (c) predicted by CNN; (d) predicted by the hierarchical learning method

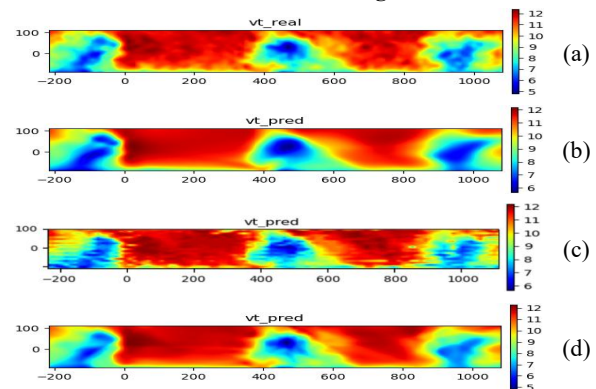


Fig. 11 Cross-section of the flow field 441 m downstream

of the fourth column (turbines 10, 11, 12) of wind turbines (a) the actual flow field obtained from simulations; (b) predicted by the MLP; (c) predicted by the CNN; (d) predicted by the proposed method

To further compare the accuracy of the three methods, the five error evaluation metrics from Section 3 were used to assess the prediction accuracy of the three methods. The prediction performance in different areas of the wind farm was analyzed and compared. In these tables, v_{11} represents the resultant velocity predicted by the hierarchical learning method, v_{12} and v_{13} represent the resultant velocity predicted by MLP and CNN, respectively. The data show clearly that the hierarchical learning model accurately predicted the transverse cross-sectional velocity of the wind farm.

In Table 4, the values of the five error evaluation metrics for the hierarchical learning method are all lower than the prediction error values of the MLP and CNN, indicating higher prediction accuracy. In contrast, the MLP shows a larger minimum velocity error and a smaller maximum velocity error, resulting in a narrower predicted wind speed range. It is significantly affected by certain extreme values, leading to overall low prediction accuracy. This suggests that the MLP failed to effectively capture the turbulent structure variations within the wind farm. The maximum and minimum prediction errors of the CNN are similar to those of the longitudinal section of the wind turbine wake field, indicating that the CNN performs poorly in predicting certain velocity variation ranges and inaccurately predicts the distribution of the wake field. Therefore, we conclude that the proposed hierarchical learning model reduces the amount of training data needed while effectively capturing the turbulent structure variations in the wind farm, demonstrating superior performance.

Table 4. Velocity prediction errors 441 m downstream of the third column of wind turbines

	<i>ME</i>	<i>me</i>	<i>MAE</i>	<i>MRE</i>	<i>RMSE</i>
v_{11}	-0.241	0.512	0.210	0.0218	0.288
v_{12}	-0.342	1.465	0.316	0.0312	0.437
v_{13}	1.552	-1.744	0.288	0.0324	0.401

In Table 5, the values of the error evaluation metrics for our proposed method are all small and close to zero, with both the maximum and minimum velocity error absolute values being significantly

smaller than those of the MLP and CNN. This indicates that our proposed method effectively captures the variations in flow field structures and exhibits better predictive performance. This is because we incorporated constraints from the 3D NS equations. Additionally, when we increased the amount of training data for the MLP, the prediction accuracy did not improve and even led to increased training time, which was also the case for the CNN. This suggests that relying solely on data to learn the physical laws of the wind farm is not ideal and may even lead to greater time and resource consumption. Therefore, the hierarchical learning model based on PINN not only reduces the amount of training data and computation time but also effectively captures the dynamics and flow details of the wind farm, demonstrating superior performance.

Table 5. Velocity prediction errors 441 m downstream of the fourth column of wind turbines

	<i>ME</i>	<i>me</i>	<i>MAE</i>	<i>MRE</i>	<i>RMSE</i>
v_{11}	-0.065	0.070	0.154	0.0155	0.209
v_{12}	-0.161	0.827	0.255	0.0257	0.334
v_{13}	1.497	-1.362	0.326	0.0357	0.432

To further demonstrate the superiority of the proposed method in wind farm prediction, Section S7 of the ESM shows the streamwise velocity u , the spanwise velocity v , and the vertical velocity w at a specific moment in the wind farm. Comparisons reveal that our hierarchical learning model based on PINNs, when compared to the MLP and CNN, can accurately predict the evolution details of velocities in each direction, capture the dependencies between three-dimensional wind speeds, and accurately forecast the short-term wake field. To validate the accuracy of the proposed hierarchical learning prediction method for each wind speed component, we conducted an analytical comparison with both MLP and CNN approaches. Detailed information is provided in Section S8 of the ESM.

4.3 Wind direction prediction error in array flow fields

To comprehensively evaluate the performance improvement of the hierarchical learning model in wind farm prediction, a comprehensive assessment of the wind direction prediction performance was undertaken. Owing to the periodic characteristic of wind direction, the ME and me are susceptible to

distortion from extreme values and offer limited insight into model consistency. Therefore, only the MAE, MRE, and RMSE were used to ensure a representative and stable evaluation of wind direction prediction performance. To ensure a robust evaluation and mitigate the risk of overfitting to a specific flow regime, the analysis targeted four strategically selected regions characterized by distinct wake interactions: the vertical cross-sections at the second row, the vertical cross-sections at the third row, the horizontal cross-section 441 m downstream of the third column, and the horizontal cross-section 441 m downstream of the fourth column. This multi-region approach effectively demonstrated the model's superior generalization capability.

The wind direction prediction errors across the four strategically selected regions are summarized in Section S9 of the ESM.

5 Conclusions

To achieve accurate prediction of wind turbine wake fields, we applied a layered learning approach within an integrated neural network framework, proposing a real-time dynamic wind field prediction method that balances both global and local aspects. By incorporating layered learning and partial differential equations, the method reconstructs dynamic wake fields at any spatiotemporal coordinates using sparse data. Simulation results showed that the proposed method has a lower algorithmic complexity, which achieves reliable prediction accuracy while reducing data requirements, effectively capturing the correlations and dependencies among wind speeds in various dimensions of the wind farm.

Although our proposed method shows high predictive accuracy and achieves a lower MAE than the other two methods, several limitations remain. First, while our hierarchical approach significantly reduces the quantity of training data required, the model's performance is ultimately dependent on the quality and representativeness of the high-fidelity simulation data used for pre-training. In practical applications where real measurement data are sparse or contaminated with noise, or when encountering inflow conditions and turbine operating states not covered in the simulation database, the model's

generalization capability and prediction accuracy may be compromised. Second, concerning physical assumptions, the physical constraints are governed by the NS equations with a fixed effective Reynolds number (Re). While this provides a valuable physical prior, it introduces simplifications. The use of a constant Re may not fully capture the dynamic, multi-scale nature of atmospheric turbulence. Furthermore, the accuracy of the model is inherently limited in regions with large velocity fluctuations and strong shear, where the assumptions underlying the NS equations might be less effective in representing complex, high-frequency turbulent structures. Third, the physical constraint component of PINNs is challenging for parallelization, which may become a computational bottleneck and hinder scalability.

Future work will focus on investigating the spatiotemporal reconstruction and prediction of wind turbine wakes in 3D space by exploring other deep neural network architectures to capture detailed changes in the near-wake and far-wake regions. Additionally, enhancing the scalability of PINNs through operator learning or sparse modeling will be explored as a complementary direction. These advancements are expected to bring significant breakthroughs and progress to the research and practical applications in the wind energy field.

Acknowledgments

This work was supported in part by the National Natural Science Foundation of China (Project 62201226) and the Guangdong Basic and Applied Basic Research Foundation (Projects 2022A1515240021).

Author contributions

Shanxun SUN designed the research. Zijiang XU and Zhuoheng WANG processed the corresponding data. Zhuoheng WANG and Shuangshuang CUI wrote the first draft of the manuscript. Ting HE and Yang CAI helped to organize the manuscript. Zijiang XU and Shanxun SUN revised and edited the final version.

Conflict of interest

Shanxun SUN, Zijiang XU, Zhuoheng WANG, Shuangshuang CUI, Ting HE and Yang CAI declare that they have no conflict of interest.

References

Amiri MM, Shadman M, Estefen SF, 2024. A review of physical and numerical modeling techniques for horizontal-axis wind turbine wakes. *Renewable and*

- Sustainable Energy Reviews*, 193:114279.
- Bai H, Wang N, Wan D, 2023. Numerical study of aerodynamic performance of horizontal axis dual-rotor wind turbine under atmospheric boundary layers. *Ocean engineering*, 280:114944.
- Bastankhah M, Porté-Agel F, 2014. A new analytical model for wind-turbine wakes. *Renewable energy*, 70:116-123.
- Frandsen S, Barthelmie R, Pryor S, et al., 2006. Analytical modelling of wind speed deficit in large offshore wind farms. *Wind Energy: An International Journal for Progress and Applications in Wind Power Conversion Technology*, 9(1-2):39-53.
- He R, Yang H, Sun H, et al., 2021. A novel three-dimensional wake model based on anisotropic gaussian distribution for wind turbine wakes. *Applied Energy*, 296:117059.
- Jensen NO, 1983. A note on wind generator interaction. translators, Risø National Laboratory,
- Li S, Zhang M, Piggott MD, 2023. End-to-end wind turbine wake modelling with deep graph representation learning. *Applied Energy*, 339:120928.
- Liu R, Peng L, Huang G, et al., 2023. A monte carlo simulation method for probabilistic evaluation of annual energy production of wind farm considering wind flow model and wake effect. *Energy Conversion and Management*, 292:117355.
- Purohit S, Ng EYK, Kabir IFSA, 2022. Evaluation of three potential machine learning algorithms for predicting the velocity and turbulence intensity of a wind turbine wake. *Renewable energy*, 184:405-420.
- Song J, Wang L, Xin Z, et al., 2025. Wake field prediction of a wind farm based on a physics-informed neural network with different spatiotemporal prediction performance improvement strategies. *Theoretical and Applied Mechanics Letters*, 15(2):100577.
- Songyue L, Qiusheng L, Bin L, et al., 2025. Prediction of offshore wind turbine wake and output power using large eddy simulation and convolutional neural network. *Energy Conversion and Management*, 324:119326.
- Sun H, Qiu C, Lu L, et al., 2020. Wind turbine power modelling and optimization using artificial neural network with wind field experimental data. *Applied Energy*, 280:115880.
- Sun S, Liu S, Liu J, et al., 2018. Wind field reconstruction using inverse process with optimal sensor placement. *IEEE Transactions on Sustainable Energy*, 10(3):1290-1299.
- Sun S, Liu S, Chen M, et al., 2019. An optimized sensing arrangement in wind field reconstruction using cfd and pod. *IEEE Transactions on Sustainable Energy*, 11(4):2449-2456.
- Sun S, Cui S, He T, et al., 2024. An integrated deep neural network framework for predicting the wake flow in the wind field. *Energy*, 291:130400.
- Wang J, Yin X, Liu Y, et al., 2023. Optimal design of combined operations of wind power-pumped storage-hydrogen energy storage based on deep learning. *Electric Power Systems Research*, 218:109216.
- Wang L, Chen M, Luo Z, et al., 2024a. Dynamic wake field reconstruction of wind turbine through physics-informed neural network and sparse lidar data. *Energy*, 291:130401.
- Wang L, Dong M, Yang J, et al., 2024b. Wind turbine wakes modeling and applications: Past, present, and future. *Ocean engineering*, 309:118508.
- Wei D, Zhao W, Wan D, et al., 2021. A new method for simulating multiple wind turbine wakes under yawed conditions. *Ocean engineering*, 239:109832.
- Xu S, Zhuang T, Zhao W, et al., 2023. Numerical investigation of aerodynamic responses and wake characteristics of a floating offshore wind turbine under atmospheric boundary layer inflows. *Ocean engineering*, 279:114527.
- Xu S, Yang X, Zhao W, et al., 2024. Numerical analysis of aero-hydrodynamic wake flows of a floating offshore wind turbine subjected to atmospheric turbulence inflows. *Ocean engineering*, 300:117498.
- Zhan L, Wang Z, Chen Y, et al., 2024. Ada2mf: Dual-adaptive multi-fidelity neural network approach and its application in wind turbine wake prediction. *Engineering Applications of Artificial Intelligence*, 137:109061.
- Zhang J, Zhao X, 2021. Spatiotemporal wind field prediction based on physics-informed deep learning and lidar measurements. *Applied Energy*, 288:116641.
- Zhou L, Wen J, Wang Z, et al., 2023. High-fidelity wind turbine wake velocity prediction by surrogate model based on d-pod and lstm. *Energy*, 275:127525.

Electronic supplementary materials

Sections S1-S9